
Research Article

Theoretical and Experimental Studies of the Controlled Release of Tetracycline Incorporated into Bioactive Glasses

Ângela L. Andrade,¹ Isabela A. Militani,² Katia J. de Almeida,² Jadson C. Belchior,³ Sérgio C. dos Reis,⁴ Rosângela M. F. Costa e Silva,³ and Rosana Z. Domingues^{3,5}

Received 27 September 2017; accepted 27 November 2017; published online 9 January 2018

Abstract. Several authors have studied the release profile of drugs incorporated in different devices. However, to the best of our knowledge, although many studies have been done on the release of tetracycline, in these release devices, no study has investigated if the released compound is actually the tetracycline, or, instead, a degraded product. This approach is exploited here. In this work, we analyse the influence of two drying methods on the tetracycline delivery behaviour of synthesised glasses using the sol-gel process. We compare the drying methods results using both theoretical models and practical essays, and analyse the chemical characteristic of the released product in order to verify if it remains tetracycline. Samples were freeze-dried or dried in an oven at 37°C and characterised by several methods such as Fourier transform infrared spectroscopy (FTIR), scanning electron microscopy (SEM), thermogravimetric analysis (TG), differential thermogravimetric analysis (DTG), differential thermal analyses (DTA) and gas adsorption analysis (BET). The released concentration of tetracycline hydrochloride was studied as a function of time, and it was measured by ultraviolet spectrophotometry in the tetracycline wavelength. The drug delivery profiles were reasonably consistent with a diffusion model analysis. In addition, we observed higher release rates for the freeze-dried compared to those dried in an oven at 37°C. This higher release can be attributed to larger pore size for the freeze-dried sample systems with tetracycline, which promoted more water penetration, improving the drug diffusion. The analysis of the solution obtained in the release tests using high-performance liquid chromatography- mass spectrometry (HPLC-MS) confirmed that tetracycline was being released.

KEY WORDS: release drug; drying; diffusion model; glass; tetracycline.

INTRODUCTION

In bone reconstruction surgery, osteomyelitis caused by bacterial infection is the most important complication. Conventional treatments include systemic antibiotic administration; however, success in therapy has not been overwhelming as with other disease conditions. Key issues for failure

include the inability to maximise drug access to bone and maintain optimum drug concentration for prolonged periods of time (1). One way of addressing this problem is the administration of anti-inflammatory and/or antibiotic drugs at the target site. This type of drug administration is not always simple, often requiring specific drug delivery systems. Several authors have studied the release profile of different drugs of such systems (including commonly used polymers and different glass compositions) (2–4). However, to our knowledge, no research has verified the chemical properties of the released substances. It might be an open question of whether the administered drugs remain in their original form or as other compounds, resulting from their degradation. Many of the techniques used to quantify the delivered drug, such as ultraviolet spectrophotometry, cannot distinguish between the original compound and its degradation products. Characterisation of the compounds actually delivered by different drug delivery systems can help in understanding loss of therapeutic activity and toxic patient responses related to possible degradation products (5). Motivated by these

¹ Departamento de Química, ICEB, Universidade Federal de Ouro Preto, UFOP, Morro do Cruzeiro, sn, Ouro Preto, MG (35.400-000), Brazil.

² Departamento de Química, Universidade Federal de Lavras, UFLA, Campus Universitário, CP 3037, Lavras, MG (37200-000), Brazil.

³ Departamento de Química, ICEX, Universidade Federal de Minas Gerais, UFMG, Av. Antônio Carlos, 6627, Belo Horizonte, MG (31.270-901), Brazil.

⁴ Centro de Desenvolvimento da Tecnologia Nuclear, CDTN/CNEN, Av. Antônio Carlos, 6627, Belo Horizonte, MG (31.270-901), Brazil.

⁵ To whom correspondence should be addressed. (e-mail: rosanazd@ufmg.br)

considerations, we undertook the task of exploring this important issue.

In previous studies, our group has pointed out the efficiency of a new device for the release of tetracycline hydrochloride incorporated in silica-based bioactive glassy systems synthesised at room temperature (2,3), without the addition of a polymer. Glassy synthesis at lower temperatures is essential since it makes possible the addition of heat-sensitive drugs. The incorporation of growth factors or antibiotics is only possible if low temperatures can be maintained throughout the process.

Mathematical models and simulations have been widely applied to study drug release from different drug delivery systems (6–9). Among several important contributions, the determination of diffusion coefficients has been particularly useful. Narasimhan (10) developed a model for polymer dissolution based on the molecular mechanism. The model describes solute transport in a one-dimensional system, such as a film, slab, disk or tablet. To investigate the effect of various parameters on the drug release behaviour, the normalised drug release as a function of time is usually simulated using drugs of different molecular sizes. An increasing rate of drug release can be observed when the drug diffusion coefficient is higher. Similarly, we have used Fick's law to determine the diffusion coefficients for two drug delivery systems (11,12).

In the present work, we describe the low-temperature synthesis and preparation of tetracycline (TC) delivery systems using a glassy matrix incorporating two different drying methods. We analyse the delivery profile and the chemical identity of the released product. Similarly, analyses about the nature of material porous were carried out. Finally, theoretical studies have provided insights about the interaction of TC with the glass and the calculation of the drug diffusion coefficients were done.

MATERIALS AND METHODS

Glass Synthesis

The synthesis procedure used to prepare the bioactive glass samples, with composition $(\text{SiO}_2)_{0.80}(\text{P}_2\text{O}_5)_{0.04}(\text{CaO})_{0.16}$, was described in detail in reference (2,3). Essentially, the process consisted in adding the precursor reagents to an aqueous HCl solution at pH 1.7 containing ethanol. First, tetraethoxysilane (TEOS) was mixed into the solution and stirred for 30 min. Next, triethylphosphate was added and stirred for another 30 min. After that, calcium chloride was added and dissolved. All of the reagents (Fluka) were of analytical grade. The molar ratio of the TEOS/ethanol and TEOS/HCl solutions was 1:4 in both cases. For samples containing tetracycline (TC), 0.144 g of tetracycline hydrochloride (Fluka Production GmbH, Germany) was added to the solution and stirred for 30 min after the addition of calcium chloride. The solution was continuously and slowly stirred until the gelation process hindered the stirring. Control samples without the drug were also prepared using the same procedure.

All samples were placed in a humidified atmosphere for 12 h.

After this period, the glass sample, with and without the drug, was withdrawn. The amount of tetracycline remaining in the vessel, *i.e.* not incorporated into the glass, was determined by ultraviolet spectrophotometry at the TC (270 nm) wavelength (2,3).

Then, 10 mL of pure acetone was added to wash the samples and quickly removed by filtration. This acetone-drying step helps to remove organic solvents released during the TEOS hydrolysis. The obtained material was divided into two parts: one portion was humidified, frozen with liquid nitrogen and freeze-dried for 24 h. The other part was dried in an oven at 37°C for 7 days. After these steps, the gels were manually crushed in an agate mortar, and powders of particle size < 1 mm were selected. All test samples were kept in the dark to avoid the photodecomposition of TC.

The samples without the drug (control group) were labelled BGF and BGO for freeze-dried and oven-dried samples, respectively. Samples containing TC were similarly named BGF-T and BGO-T. The initial TC percentage (wt%) was approximately 2% for all samples.

Drug Release

Cylindrical pellets were prepared for drug delivery tests by compressing about 0.25 g of powder, either with or without TC, at a 1300-ton loading for 3 min (2,3). These conditions were used because they were suitable for compacting the samples. This procedure produced pellets with, on average, a radius of 6.98 mm and a length 4.15 mm.

The release profile was determined as follows. Test samples were placed into polystyrene bottles containing 3 mL of simulated body fluid (SBF) (13) and incubated at 37°C. Aliquots were withdrawn and analysed by ultraviolet spectrophotometry at the TC (270 nm) wavelength (2,3).

At predefined time points throughout the study, the SBF was replaced with fresh solution. All samples were analysed in triplicate. Samples without the drug were used as controls.

For the purpose of the study of the stability of the liberated tetracycline, the solution released from the samples with tetracycline was analysed by HPLC-MS. For this, a part of the cylindrical pellets of the BGF-T and BGO-T samples was placed in 3 mL of water and treated with ultrasound for 5 min. The supernatant was removed and injected into a C18 cartridge which had been preconditioned with methanol (5 mL), followed by three washes with Milli-Q water (3×5 mL). Several solvents such as water and methanol were trialled for the extraction. As tetracycline hydrochloride possesses both acid and alkaline properties, ammonium hydroxide and formic acid were used to improve its ionisation. The study was performed in both positive and negative ion modes. Methanol and formic acid resulted in the highest extraction efficiency. An important problem in the quantitative analysis of TC is that it has been shown to chelate metals. Thus, it may irreversibly bind residual metals on SPE cartridges, lowering recovery (14,15). As we were aiming to perform only a qualitative analysis in this work, the irreversibly bound fraction could be ignored.

Aliquots obtained from the solid-phase extraction were analysed by MS. The operational parameters for TC were carefully optimised.

The stock solution of TC was directly infused along with the mobile phase into the MS. Optimisation of the mass parameters was performed by observing the maximum response obtained for the selected product.

Theoretical Modelling

The interactions of TC with the glass were simulated using a computational model where the direct interactions of bioactive glass with TC were taken into account. Figure 1 shows the sites of TC, which were considered to interact directly with Si(O)₄. This model has been successfully used to describe the most important interactions of TC with essential or non-essential systems in previous works (16–19). The long-distance interaction effects were evaluated using the polarised continuum model by means of the PCM method (20). Full geometry optimisation and vibrational frequency calculations were performed without restriction using density functional theory (DFT) together with the hybrid B3LYP function (21–23). The standard TZVP basis sets were employed for all atoms (24). The GEDIIS algorithm (19) was employed throughout; the final structures were obtained with tight SCF and geometry convergence criteria in combination with the ultrafine integration grid. Frequency calculations were performed to confirm the nature of each stationary point, which also afforded zero-point energy (ZPE) corrections for the computed energies. The GAUSSIAN 09 program package was used for all calculations.

In addition, Fick's law was used to obtain the diffusion coefficients for the pellets BGF-T and BGO-T. The pellets were cylindrical with radius *a* and length *l*. For this specified geometry, the following differential equation can be solved (10,11,25):

$$\frac{\partial C}{\partial t} = D \left[\frac{\partial^2 C}{\partial r^2} + \frac{1}{r} \frac{\partial C}{\partial r} + \frac{\partial^2 C}{\partial z^2} \right] \quad (1)$$

where *D* is the diffusion coefficient, *C* is the concentration and *r* and *z* are variables defined within the limits $0 \leq r \leq a$ and $-l \leq z \leq l$, respectively. The solution of such an equation can be written as:

$$C = C_0 \psi(z) \phi(r, a) \quad (2)$$

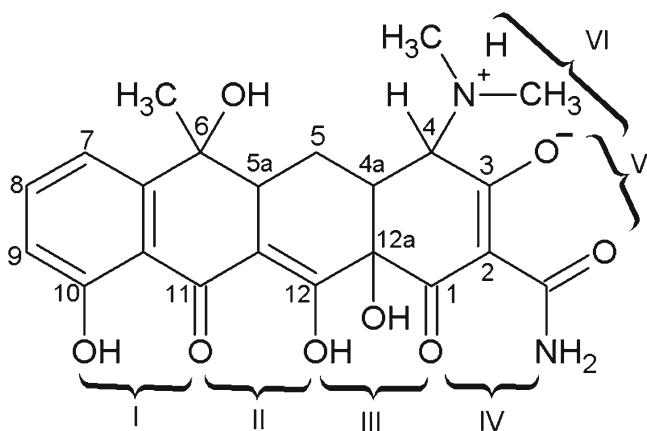


Fig. 1. Molecular structure of tetracycline (TC) indicating direct interaction sites

where *C*₀ is the initial concentration and $\psi(z)$ and $\phi(r, a)$ are the auxiliary functions:

$$\psi(z) = \frac{4}{n} \sum_{n=0}^{\infty} \frac{(-1)^n}{(2n+1)} \exp \left[-D(2n+1)^2 \frac{\pi^2 t}{4l^2} \right] \times \cos \frac{(2n+1)\pi}{2l} Z \quad (3)$$

and:

$$\phi(r, a) = \frac{2}{a} \sum_{m=1}^{\infty} \exp(-Da_m^2 t) \frac{J_0(ra_m)}{a_m J_1(ra_m)} \quad (4)$$

where *J*₀(*x*) and *J*₁(*x*) are Bessel functions of order zero and one, respectively. Since the available experimental data is the fraction of drug fraction release (*F*), we use:

$$F = \frac{M(t)}{M(\infty)} = 1 - \frac{8}{l^2 a^2} \sum_{m=1}^{\infty} \frac{\exp(-Da_m^2 t)}{a_m^2} \sum_{n=0}^{\infty} \frac{\exp(-D\beta_n^2 t)}{\beta_n^2} \quad (5)$$

where $\beta = (2n+1)\pi/(2l)$ and α_m are the roots of Bessel functions. One may assume that the device is not consumed, and the parameter *a* will approach infinity as time increases. In this case, the above equation leads to:

$$F = 1 - 8 \sum_{n=0}^{\infty} \frac{\exp(-D(2n+1)^2 \pi^2 t / 4l^2)}{(2n+1)^2 \pi^2} \quad (6)$$

This equation is used in a nonlinear least-squares fit to the experimental data using the Marquardt-Levenberg algorithm (26) to extract the diffusion coefficient.

Characterisation Methods

Sample structure and homogeneity were characterised by comparison of FTIR spectra obtained in a Perkin Elmer Spectrum GX spectrophotometer. For these analyses, the solids were homogeneously dispersed in KBr (approximately 1 wt%) and pressed into discs. Spectra were recorded with a resolution of 4 cm⁻¹ with 32 scans per spectrum. Sample morphology was studied by scanning electron microscopy (SEM) (Quanta 200 FEI). Prior to analysis, the samples were fastened to a sample holder with the help of a double carbon ribbon and covered with gold. Thermogravimetric (TG), differential thermogravimetric (DTG) and differential thermal analyses (DTA) were carried out in a Shimadzu DTG-60 H thermal analyser from 25 to 900°C at 10°C/min in air. Al₂O₃ was used as a standard.

Gas adsorption analysis (BET-Nova-2200, Quantachrome Corporation) was used to study the specific surface area and the micro- and mesoporosity of the materials. The powders were accurately weighed using an FA2104 electronic balance with 0.1 mg precision. Before measurement, all samples were degassed at 60°C for 24 h.

The released solution containing TC was analysed using an HPLC-MS system. The LC equipment used was a

Shimadzu® LCMS-IT-TOF (225-07100-34). The mobile phase was a mixture of water and methanol (1:1) and the flow rate was 0.15 mL min^{-1} . The injection volume was $20 \mu\text{L}$. The MS was operated in positive and negative electrospray ionisation (ESI) modes using the following conditions: electrospray voltage of 1.76 kV, block and CDL temperature of 200°C and capillary tension of 4.5 kV. Samples were fully scanned in the mass range 200 to 500 m/z. The qualifier ions of the TC were 445.1605 m/z (precursor ion, $[\text{M} + \text{H}]^+$), 428.4340 and 410.4234 m/z (fragment ion).

RESULTS AND DISCUSSION

SEM micrographs of oven-dried samples and of freeze-dried samples, with or without TC (BGO, BGO-T, BGF and BGF-T, respectively), before and after immersion in SBF are shown in Figs. 2 and 3. The BGO surface is irregular and no pores at all can be seen (Fig. 2a). The oven-dried sample containing TC, BGO-T, (Fig. 2b) shows many irregularities and pores before immersion, probably due to adsorbed water bound to TC molecules. After immersion in SBF these samples (Fig. 2c, d) become more irregular mainly through erosion. In contrast, samples prepared by freeze-drying, without or with TC (BGF and BGF-T, respectively), before and after immersion in SBF (Fig. 3a, d) exhibit many pores.

The freeze-dried samples present large pore diameters, probably due to the more efficient drying process. This particular behaviour has been also reported in the literature (27–29). In these works, the authors demonstrated that the drying step can cause the volumetric contraction of oven-dried pellets. The biggest difference in diameter appears when freezing occurs rapidly by immersion in liquid nitrogen.

FTIR spectra of all glass samples before immersion in SBF, either with or without TC (Fig. 4), are very similar, probably due to the effective incorporation of the drug. Previous studies have shown that the presence of a drug inside a delivery system, rather than interacting at the surface, could explain the similarity of FTIR spectra of isolated and immobilised drug-delivery systems (30,31). The absorption bands at 1080 , 800 and 460 cm^{-1} are due to Si–O–Si bonds (32–34), and the peaks at 940 cm^{-1} can be attributed to Si–OH bond vibrations (35).

The dosage of tetracycline remaining in the vessel after removal of the glass-tetracycline composite showed that about 0.1% of the tetracycline added to the glass during its synthesis was not incorporated.

The influence of the two drying methods on the TC release profile is shown in Fig. 5.

In this Figure, it can be observed that, initially, there is a fast release. Although the significance of burst release in

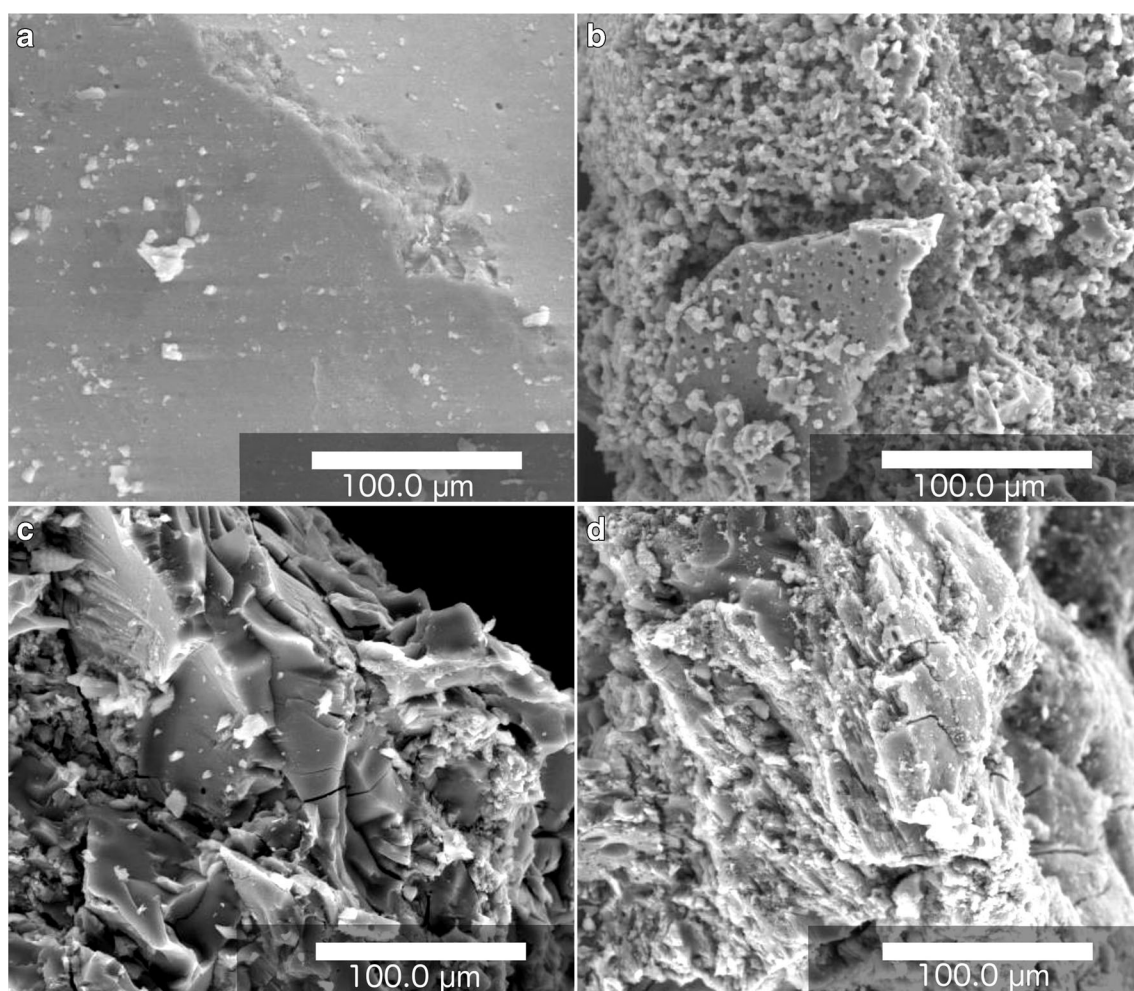


Fig. 2. SEM images of oven-dried samples before: **a** BGO, **b** BGO-T, and after immersion in SBF for 9 h: **c** BGO, **d** BGO-T

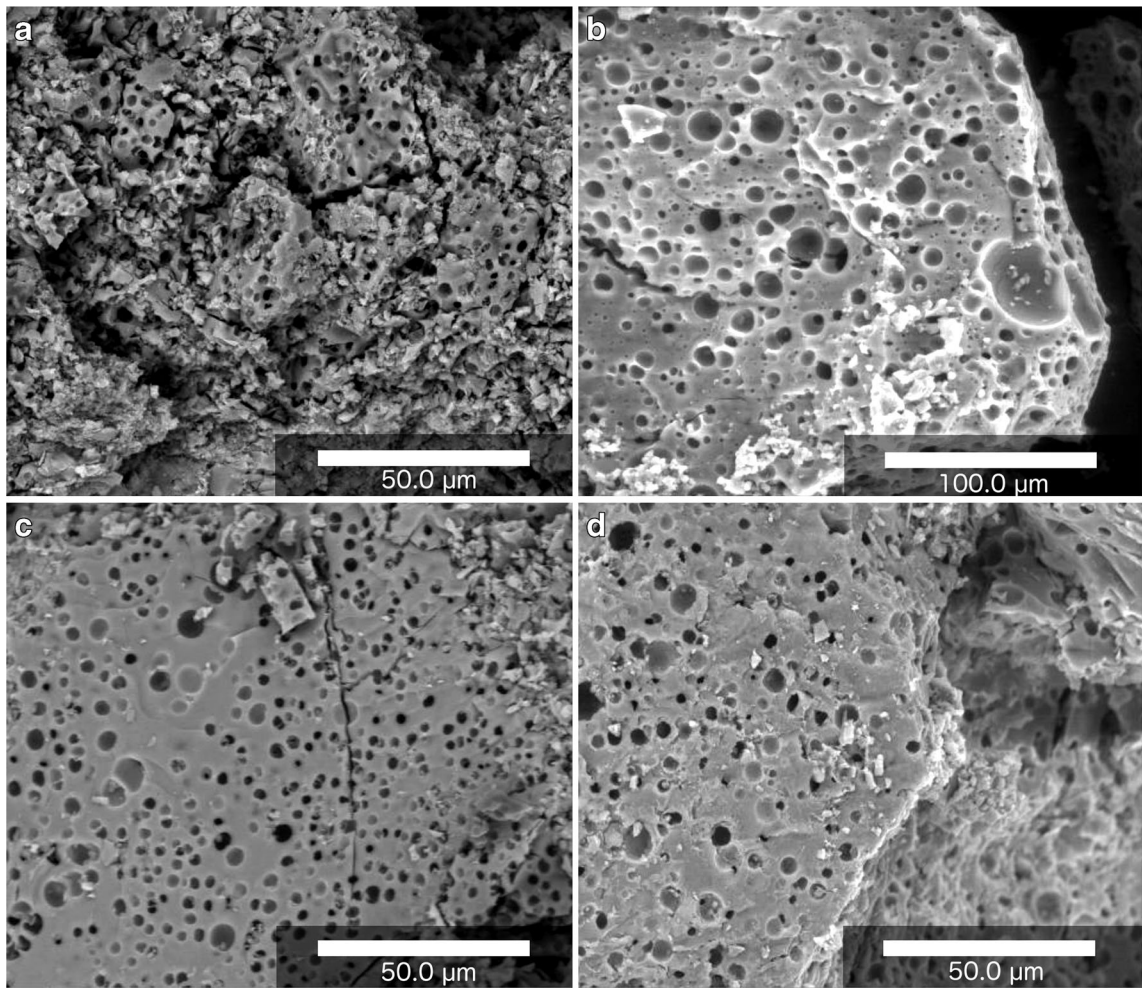


Fig. 3. TEM images of freeze-dried samples before: **a** BGF, **b** BGF-T, and after immersion in SBF for 9 h: **c** BGF, **d** BGF-T

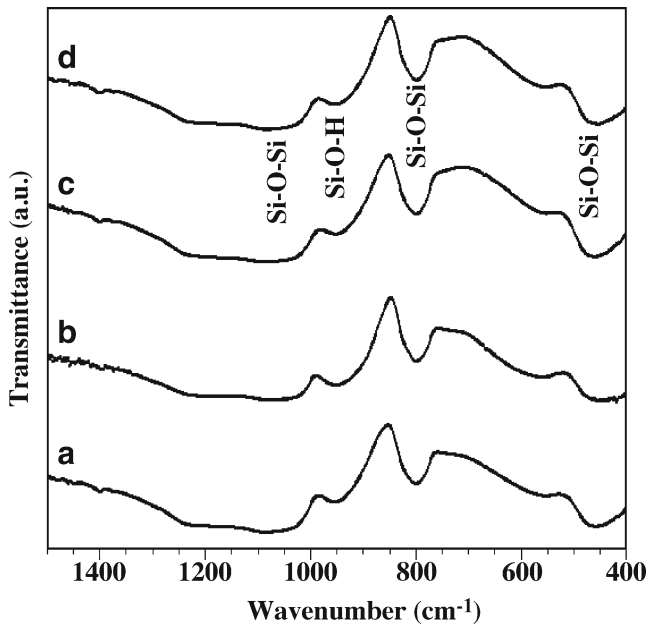


Fig. 4. FTIR spectra of samples: (A) BGO, (B) BGO-T, (C) BGF and (D) BGF-T, before immersion in SBF

controlled delivery systems has been slightly addressed in the literature, no successful theories have been put forth to fully

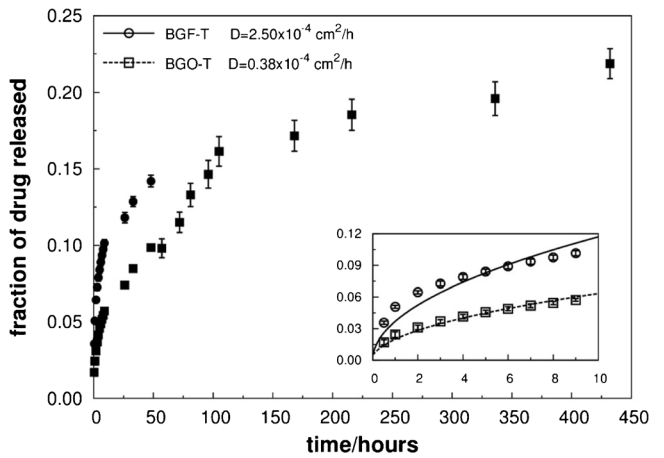


Fig. 5. Fraction of tetracycline released from the samples BGF-T and BGO-T as a function of time. The first 10 h of release was modelled to obtain the diffusion coefficients

Table I. The B3LYP/TZVP Energies (ΔE) for the Formation of TC-Si(OH)₂ Systems, in Kilocalories per Mole

TC-Si(OH) ₂	
Systems	ΔE (in kcal mol ⁻¹)
Gas phase	
I	-4.02
II	-1.38
III	48.12
IV	7.38
V	-39.98
VI	26.32
Water PCM solvent	
I	5.33
II	2.50
III	46.70
IV	4.08
V	-27.78
VI	14.75

describe the phenomenon (36). One suggested explanation for the burst effect in monolithic systems is that some drug becomes trapped on the surface of the polymer matrix during the manufacturing process (37), especially in the case of high drug loading (38), and is released immediately upon activation in a release medium. When released devices are loaded with drugs by equilibrium partitioning in highly concentration drug solutions, this phenomenon may happen (39).

Figure 5 also shows that the freeze-dried sample presents more efficient drug release. According to other authors (27,29,40), this may be expected since this sample is more porous compared with the 37°C oven-dried sample as shown by MEV in Figs. 2 and 3. Pore size appears to be a critical factor for achieving controlled release; the greater the pore size, the faster the entrance of water and, consequently, the faster the drug release.

The release profile shows two stages. The first stage corresponds to rapid early release of the drug. A release of 6 and 10% of the TC in the first 9 h was observed for BGO-T and BGF-T, respectively. This rapid release can be explained by the porous structure of the samples (the release rate depending on the pore size, shape and connectivity). In the second stage, a more controlled and slower behaviour is observed for TC release. These features suggest a relatively weak interaction between TC and the glasses. We further

Table II. Structural Parameters, Specific Surface Area (S_{BET}) and Total Pore Volume (V_{P}) of the BGO, BGF, BGO-T and BGF-T Samples before Immersion in SBF

Samples	S_{BET} (m ² /g)	V_{P} (cm ³ /g)
BGO	95.2238	0.22119
BGF	15.8707	0.05909
BGO-T	1.4183	0.00691
BGF-T	1.3348	0.00521

investigated these interactions using theoretical analyses. The most stable structures of the optimised TC-Si(O)_n systems were used to provide the energies of formation for each interaction site of TC with glass. The obtained results are shown in Table I, where the B3LYP/TZVP values were computed in the gas-phase and aqueous solution phases. As can be seen in Table I, all interaction modes were stabilised in both phases. Overall, the optimised structures converged, forming intramolecular hydrogen interactions. The energy results obtained for the gas-phase indicate that interactions involving sites I, II and V are favoured from a thermodynamic point of view, showing B3LYP/TZVP values varying from -1.38 to -39.98 kcal mol⁻¹. However, when solvent effects are taken into account, only the interaction with site V remains exothermic at -27.78 kcal mol⁻¹.

The computed energies in water lie above 15 kcal mol⁻¹, with only one exception observed for site III, which shows an interaction energy of 46.70 kcal mol⁻¹. These results indicate some noteworthy features, which can be used for interpretation of the experimental findings. First, a relatively weak chemical interaction may, in fact, occur between TC and glass. Another point is that the interactions between TC and glass appear to be quite dependent on environmental factors such as the solvent, pH and temperature. It is important to note that a successful delivery system may be manufactured only if the interactions between the drug and release dispositive are favoured in the synthetic process, but in such a way that delivery at the target site is not thermodynamically unfavourable. Considering these factors, the obtained theoretical insights are in good agreement with the experimental results, which shows a rapid initial release, followed by a slower release.

In order to obtain the diffusion coefficients, Eq. (6) was used to fit the experimental data for the region where the model is most efficient, during the first 9 h of release. The summation was truncated at the highest number of terms, although we have verified that the use of a minimum of six terms would be sufficient to converge to the values reported here. The calculated diffusion coefficients are 2.5×10^{-4} cm²/h for BGF-T and 0.38×10^{-4} cm²/h for BGO-T. The theoretical results are also in agreement, demonstrating that the freeze-dried pellet produces a faster release profile compared with the sample dried in an oven at 37°C. In most cases, drug release from a porous carrier is primarily diffusion controlled, the apparent drug diffusivity depending on the pore size as also verified in ref. (41). As pointed out by Narasimhan and Peppas (42), a higher drug diffusion coefficient in the samples usually produces a greater drug release.

The size of pores present in different materials covers the wide range of values, from micro- (pores with sizes smaller than 2 nm) to macropores (pores with sizes larger than 50 nm). In order to determine the possible applications of the present materials, the knowledge of parameters such as specific surface, pore volume, *etc.*, is of great interest. In the sol-gel processes, the formed gel is constituted by cross-linked structures giving rise to a porous development. Inside the pores of the gel one can detect alcohol, water, *etc.*, that are occluded. Such liquids are eliminated along the drying phase of the gel. In such step, contraction and hardening of the gel occur. As can be observed in the present study, drying of the two glasses was successfully obtained by different processes.

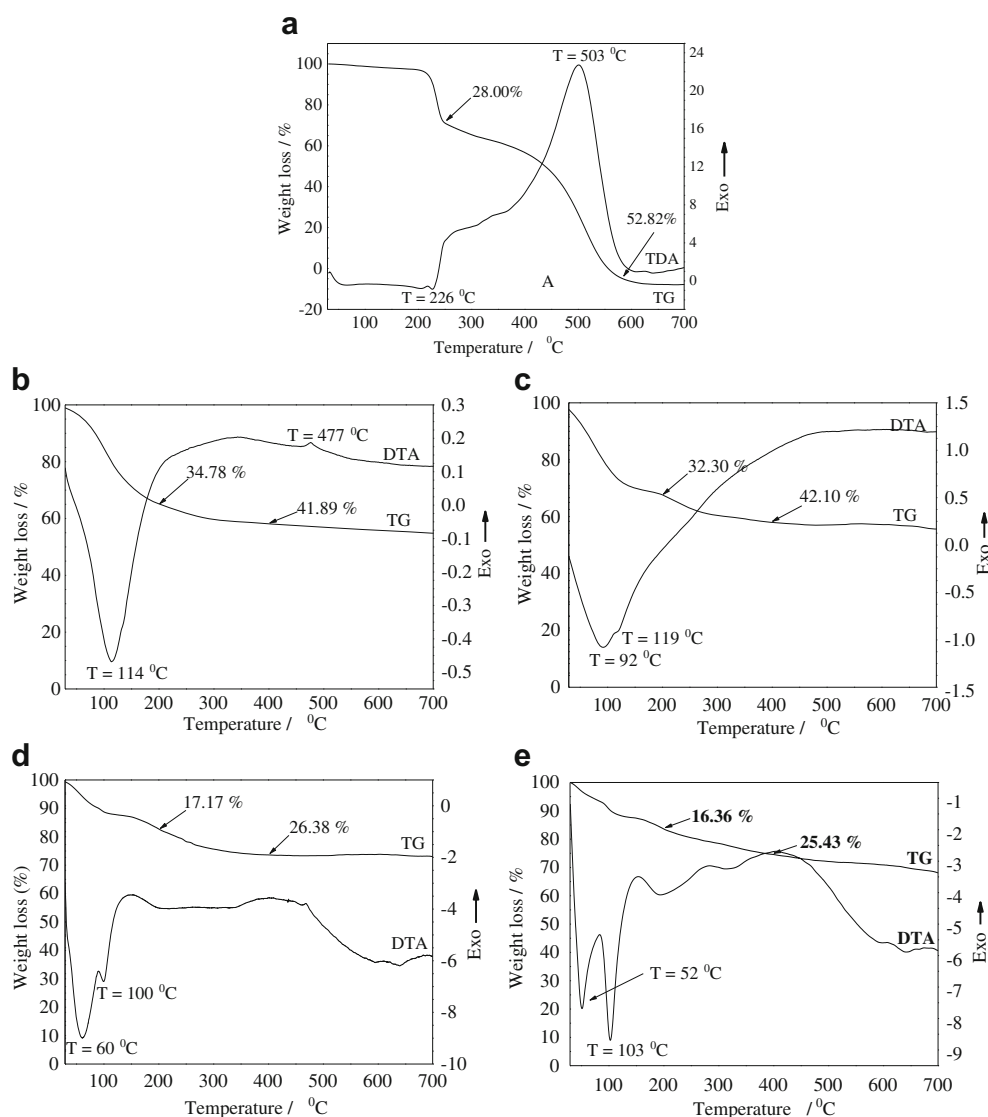


Fig. 6. TGA/DTA diagrams of samples: **a** tetracycline, **b** BGO, **c** BGO-T, **d** BGF and **e** BGF-T, before immersion in SBF. The initial tetracycline percentage (wt%) was approximately 2% for all samples

Therefore, products with different porosities may have been formed, which may have changed the tetracycline release profile.

The physicochemical parameters surface area (S_{BET}) and total pore volume (V_{P}) are shown in Table II. If we compare the BGO and BGF samples without TC, and before the test release, one can observe that the drying process drastically alters these parameters (Table II). For example, the S_{BET} for BGO is more than six times higher than for BGF. Similarly, V_{P} is higher by a factor of seven. On the other hand, in the samples incorporating TC, there is no great difference. Since the nitrogen adsorption technique (BET method) characterises meso- and micropores (43), we can observe that the oven-dried sample presents more meso- and micropores than the freeze-dried sample. However, it can be observed that these properties are decreased after loading of the drug and before the test

release, confirming that TC has been loaded into the samples (Table II). A comparison of samples BGO-T and BGF-T before immersion in SBF demonstrates that the specific surface area and total pore volume are very similar. This result leads us to conclude that micro- and mesopores do not affect the release of TC in this study. Probably macropores observed in the TEM images are responsible for the difference in each release.

The isotherms of the BGO and BGF samples before immersion in SBF (data not shown) belong to a mixed type in the IUPAC classification (44). According to this classification, our results suggest that the materials belong to type IV. In this type, the hysteresis loop is associated with capillary condensation taking place in mesopores (pores of widths between 2 and 50 nm) and its initial part corresponds to monolayer-multilayer adsorption. This observation is typical of non-porous or macroporous

materials, and represents a process of monolayer–multi-layer adsorption.

Thermogravimetric (TG) and differential thermal analysis (DTA) curves of various samples are shown in Fig. 6. The TG curve of TC (Fig. 6a) shows two mass loss events, the first starting at about 210°C and a second one at a temperature higher than 210°C. Both mass losses are attributed to thermal decomposition of the compound with formation of elemental carbon. These events correspond to an exothermic peak at about 503°C in the DTA curve. For the TG curves of samples without TC (BGO and BGF), two weight loss stages are observed (Fig. 6b, d). Similar to Ma *et al.* (2011) (45), we observed that the first weight loss occurs between the initial temperature, 30°C, and 170°C, being associated with the removal of physically adsorbed water. This corresponds to an endothermic peak at about 110°C in DTA curves. It is important, however, to observe that the BGF sample presents a smaller mass loss than the BGO sample up to 170°C (17.17 and 34.78%, respectively). This observation is evidence that the freeze-drying method is more efficient at extracting water rather than oven drying at 37°C. For samples containing TC (Fig. 6c, e), this peak in the DTA curve appears at a lower temperature, probably due to weaker interactions between residual water molecules in the glass and TC. It is again observed that the freeze-dried sample loses less mass than the oven-dried sample with values of 16.36 and 32.30%, respectively. The second weight loss starts from the end of the first weight loss (170°C) and continues up to 360°C, and it can be attributed to the loss of more volatile organics (45).

More insights into the thermal decomposition peaks can be obtained from the DTG curves (Fig. 7). The TC decomposition peak at about 225°C is probably shifted to about 100°C in the BGO-T and BGF-T glasses. This could indicate a lower thermal stability of loaded TC in comparison with isolated or pure TC.

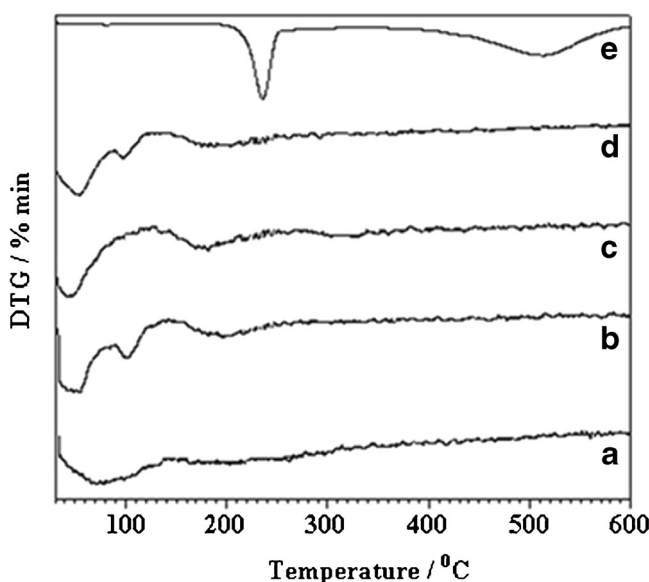


Fig. 7. DTG curves of samples: (a) BGO, (b) BGO-T, (c) BGF and (d) BGF-T before immersion in SBF, and (e) tetracycline

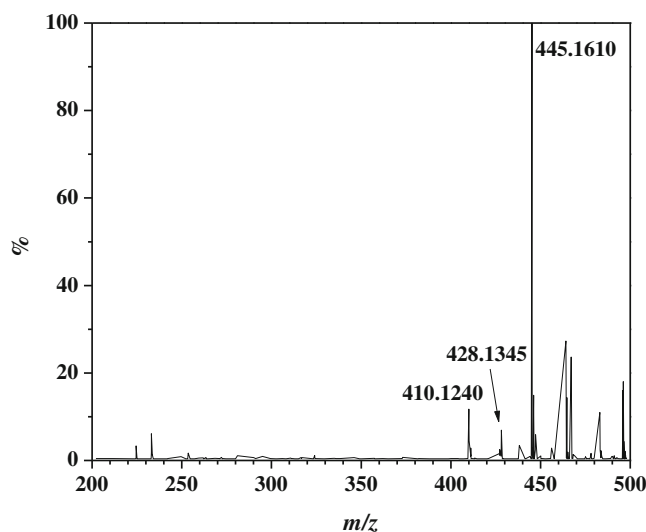


Fig. 8. Chromatogram of $[M+H]^+$, $[M+H-NH_3]^+$ and $[M+H-NH_3-H_2O]^+$ for tetracycline, indicating the products observed

In this work, TC was incorporated during glass synthesis, at pH 1.7. This incorporation was possible because we did not use high temperatures in the glass synthesis, which can degrade biologically active compounds. However, it is known that some TC, particularly chlortetracycline, rapidly isomerise in aqueous solutions of pH 2–6 at the C-4 dimethylamino group, forming 4-epitetracyclines (46). In addition, keto-enol tautomers are also rapidly formed in aqueous solution (47). Mohammed-Ali (2012) studied the effects of factors such as humidity, light and pH on the stability of TC solutions (48). He showed a change in colour over 10–20 days, from light yellow to brown and dark brown, on exposure to acidic or alkaline solutions. Thus, it is necessary to investigate whether the chemical compound released from the glass is the same TC compound as that originally loaded into the sample. HPLC-MS analysis was employed to clarify this, if the tetracycline molecule was being released intact from the glass sample.

With optimisation, it was verified that the MS response after extraction in methanol and using positive mode was higher than that after extraction in water and using negative mode. In the tetracycline spectra of the stock solution, the protonated molecular ions $[M+H]^+$ m/z 445.1605 showed a quite abundant ion peak (Fig. 8). The mass spectrum also showed losses of 17.0265 and 35.0371 Da, corresponding to m/z peaks at 428.1340 and 410.1234. The loss of 17 Da corresponded to the loss of NH_3 . The loss of 35 Da corresponded to the loss of NH_3 with a subsequent loss of H_2O . These peaks agree with the findings of other research groups (15,49,50). The m/z of the tetracycline spectrum obtained in this study was 445.1610, with an error of less than 1.5 ppm, and the released compound was the same as the drug that was originally incorporated.

In the spectra of solutions released by samples containing tetracycline, all peaks of the precursor were identified, which shows that tetracycline molecule was being released.

CONCLUSIONS

This work presents results concerning the performance of drug delivery systems based on glasses prepared by a sol-gel process. Firstly, the tetracycline was successfully incorporated into glass, and the drying process was shown to influence the morphology and homogeneity of samples, and the release of drug. In this case, the BGF-T sample demonstrated a higher fraction of released TC compared to BGO-T, probably because the freeze-dried samples were relatively more porous than those that were oven dried. Other interesting results are related to the modification of the thermal stability of tetracycline-glass samples. The isolated or pure tetracycline decomposition peak at about 225°C was shifted lower to 100°C when the drug was incorporated into glasses, indicating that the loaded tetracycline is of lower thermal stability.

Drug delivery profiles were reasonably consistent with theoretical analyses of the TC-glass interactions as well as the diffusion theoretical model. They showed that the employed synthesis of a tetracycline hydrochloride-containing glass might offer a useful way to design a controlled-release drug delivery system in freeze-dried or 37°C oven-dried samples. This study also demonstrated that higher levels of drug release are correlated with higher drug diffusion coefficients. Finally, the analysis of solutions released by samples containing tetracycline indicated that TC was released.

ACKNOWLEDGEMENTS

This work was supported by CNPq and FAPEMIG (including grant # APQ-00651-11), Brazil.

REFERENCES

- Soundrapandian C, Sa B, Datta S. Organic-inorganic composites for bone drug delivery. *AAPS PharmSciTech*. 2009;10(4):1158-71. <https://doi.org/10.1208/s12249-009-9308-0>.
- Andrade AL, Manzi D, Domingues RZ. Tetracycline and propolis incorporation and release by bioactive glassy compounds. *J Non-Cryst Solids*. 2006;352(32-35):3502-7. <https://doi.org/10.1016/j.jnoncrysol.2006.03.083>.
- Andrade AL, Souza DM, Vasconcelos WA, Ferreira RV, Domingues RZ. Tetracycline and/or hydrocortisone incorporation and release by bioactive glasses compounds. *J Non-Cryst Solids*. 2009;355(13):811-6. <https://doi.org/10.1016/j.jnoncrysol.2009.01.015>.
- Wong TW, Colombo G, Sonvico F. Pectin matrix as oral drug delivery vehicle for colon cancer treatment. *AAPS PharmSciTech*. 2011;12(1):201-14. <https://doi.org/10.1208/s12249-010-9564-z>.
- Carvalho JP, Santos AS, Sa AS, Teixeira CS, Nogueira MS. Estabilidade de medicamentos no âmbito farmacológico. *Rev Farm Med*. 2005;34:22-7.
- Frenning G, Tunon A, Alderborn G. Modelling of drug release from coated granular pellets. *J Control Release*. 2003;92(1-2):113-23. [https://doi.org/10.1016/S0168-3659\(03\)00300-6](https://doi.org/10.1016/S0168-3659(03)00300-6).
- Arifin DY, Lee LY, Wang CH. Mathematical modeling and simulation of drug release from microspheres: implications to drug delivery systems. *Adv Drug Deliv Rev*. 2006;58(12-13):1274-325. <https://doi.org/10.1016/j.addr.2006.09.007>.
- Siepmann J, Karrout Y, Gehrke M, Penz FK, Siepmann F. Predicting drug release from HPMC/lactose tablets. *Int J Pharm*. 2013;441(1-2):826-34. <https://doi.org/10.1016/j.ijpharm.2012.12.009>.
- Juncu G, Stoica-Guzun A, Stroescu M, Isopencu G, Jinga SI. Drug release kinetics from carboxymethylcellulose-bacterial cellulose composite films. *Int J Pharm*. 2016;510(2):485-92. <https://doi.org/10.1016/j.ijpharm.2015.11.053>.
- Narasimhan B, Langer R. Zero-order release of micro- and macromolecules from polymeric devices: the role of the burst effect. *J Control Release*. 1997;47(1):13-20. [https://doi.org/10.1016/S0168-3659\(96\)01611-2](https://doi.org/10.1016/S0168-3659(96)01611-2).
- Burgos AE, Belchior JC, Sinisterra RD. Controlled release of rhodium (II) carboxylates and their association complexes with cyclodextrins from hydroxyapatite matrix. *Biomaterials*. 2002;23(12):2519-26. [https://doi.org/10.1016/S0142-9612\(01\)00386-6](https://doi.org/10.1016/S0142-9612(01)00386-6).
- Reis MAA, Sinisterra RD, Belchior JC. An alternative approach based on artificial neural networks to study controlled drug release. *J Pharm Sci*. 2004;93(2):418-30. <https://doi.org/10.1002/jps.10569>.
- Kokubo T, Kushitani H, Sakka S, Kitsugi T, Yamamuro T. Solutions able to reproduce in vivo surface-structure changes in bioactive glass-ceramic A-W3. *J Biomed Mater Res*. 1990;24(6):721-34. <https://doi.org/10.1002/jbm.820240607>.
- Blanchflower WJ, McCracken RJ, Haggan AS, Kennedy DG. Confirmatory assay for the determination of tetracycline, oxytetracycline, chlortetracycline and its isomers in muscle and kidney using liquid chromatography mass spectrometry. *J Chromatogr B*. 1997;692(2):351-60. [https://doi.org/10.1016/S0378-4347\(96\)00524-5](https://doi.org/10.1016/S0378-4347(96)00524-5).
- Vartanian VH, Goolsby B, Brodbelt JS. Identification of tetracycline antibiotics by electrospray ionization in a quadrupole ion trap. *J Am Soc Mass Spectrom*. 1998;9(10):1089-98. [https://doi.org/10.1016/S1044-0305\(98\)00078-6](https://doi.org/10.1016/S1044-0305(98)00078-6).
- Lambs L, Decocklereverend B, Kozlowski H, Berthon G. Metal ion-tetracycline interactions in biological-fluids. 9. Circular-dichroism spectra of calcium and magnesium complexes with tetracycline, oxytetracycline, doxycycline, and chlortetracycline and discussion of their binding modes. *Inorg Chem*. 1988;27(17):3001-12. <https://doi.org/10.1021/ic00290a022>.
- Desiqueira JM, Carvalho S, Paniago EB, Tosi L, Beraldo H. Metal-complexes of anhydrotetracycline. 1. A spectrometric study of the Cu(II) and Ni(II) complexes. *J Pharm Sci*. 1994;83:291-5. <https://doi.org/10.1002/jps.2600830306>.
- Machado FC, Demicheli C, Garnier-Suillerot A, Beraldo H. Metal-complexes of anhydrotetracycline. 2. Absorption and circular-dichroism study of Mg(II), Al(III), and Fe(III) complexes. Possible influence of the Mg(II) complex on the toxic side-effects of tetracycline. *J Inorg Biochem*. 1995;60(3):163-73. [https://doi.org/10.1016/0162-0134\(95\)00017-1](https://doi.org/10.1016/0162-0134(95)00017-1).
- Matos SVD, Beraldo H. Metal-complexes of anhydrotetracycline. 3. An absorption and circular-dichroism study of the Ni(II), Cu(II) and Zn(II) complexes in aqueous-solution. *J Braz Chem Soc*. 1995;6(4):405-11. <https://doi.org/10.5935/0103-5053.19950069>.
- Mennucci B, Tomasi J, Cammi R, Cheeseman JR, Frisch MJ, Devlin FJ, et al. Polarizable continuum model (PCM) calculations of solvent effects on optical rotations of chiral molecules. *J Phys Chem A*. 2002;106(25):6102-13. <https://doi.org/10.1021/jp020124t>.
- Becke AD. Density-functional exchange-energy approximation with correct asymptotic-behavior. *Phys Rev A*. 1988;38(6):3098-100. <https://doi.org/10.1103/PhysRevA.38.3098>.
- Becke AD. Density-functional thermochemistry. 3. The role of exact exchange. *J Chem Phys*. 1993;98(7):5648-52. <https://doi.org/10.1063/1.464913>.
- Lee C, Yang W, Parr RG. Development of the colle-salvetti correlation-energy formula into a functional of the electron-density. *Phys Rev B*. 1988;37(2):785-9. <https://doi.org/10.1103/PhysRevB.37.785>.
- Godbout N, Salahub DR, Andzelm J, Wimmer E. Optimization of gaussian-type basis-sets for local spin-density functional calculations. 1. Boron through neon, optimization technique and validation. *Can J Chem*. 1992;70(2):560-71. <https://doi.org/10.1139/v92-079>.

25. Langer RS, Wise DL. Medical applications of controlled release, vol. I. Boca Raton: CRC-Press; 1984. p. 42–65.
26. Marquardt DW. An algorithm for least-squares estimation of nonlinear parameters. *J Soc Ind Appl Math.* 1963;11(2):431–41. <https://doi.org/10.1137/0111030>.
27. Wlosnewski JC, Kumpugdee-Vollrath M, Sriamornsak P. Effect of drying technique and disintegrant on physical properties and drug release behavior of microcrystalline cellulose-based pellets prepared by extrusion/spheronisation. *Chem Eng Res Des.* 2010;88(1):100–8. <https://doi.org/10.1016/j.cherd.2009.07.001>.
28. Gomez-Carracedo A, Souto C, Martinez-Pacheco R, Concheiro A, Gomez-Amoza JL. Microstructural and drug release properties of oven-dried and of slowly or fast frozen freeze-dried MCC-Carbopol® pellets. *Eur J Pharm Biopharm.* 2007;67(1):236–45. <https://doi.org/10.1016/j.ejpb.2007.01.006>.
29. Song B, Rough SL, Wilson DI. Effects of drying technique on extrusion–spheronisation granules and tablet properties. *Int J Pharm.* 2007;332(1–2):38–44. <https://doi.org/10.1016/j.ijpharm.2006.09.050>.
30. Jalvandi J, White M, Truong YB, Gao Y, Padhye R, Kyratzis IL. Release and antimicrobial activity of levofloxacin from composite mats of poly(ϵ -caprolactone) and mesoporous silica nanoparticles fabricated by core–shell electrospinning. *J Mater Sci.* 2015;50(24):7967–74. <https://doi.org/10.1007/s10853-015-9361-x>.
31. Tan JM, Karthivashan G, Abd Gaani S, Fakurazi S, Hussein MZ. In vitro drug release characteristic and cytotoxic activity of silibinin-loaded single walled carbon nanotubes functionalized with biocompatible polymers. *Chem Cent J.* 2016;10(1):81. <https://doi.org/10.1186/s13065-016-0228-2>.
32. Bertoluzza A, Fagnano C, Morelli MA, Gottardi V, Guglielmi M. Raman and infrared-spectra on silica-gel evolving toward glass. *J Non-Cryst Solids.* 1982;48(1):117–28. [https://doi.org/10.1016/0022-3093\(82\)90250-2](https://doi.org/10.1016/0022-3093(82)90250-2).
33. Matos MC, Ilharco LM, Almeida RM. The evolution of TEOS to silica-gel and glass by vibrational spectroscopy. *J Non-Cryst Solids.* 1992;147:232–7. [https://doi.org/10.1016/S0022-3093\(05\)80622-2](https://doi.org/10.1016/S0022-3093(05)80622-2).
34. Chu PY, Clark DE. Infrared-spectroscopy of silica sols—effects of water concentration, catalyst, and aging. *Spectrosc Lett.* 1992;25(2):201–20. <https://doi.org/10.1080/00387019208020687>.
35. Yoshino H, Kamiya K, Nasu H. IR study on the structural evolution of sol-gel derived SiO₂ gels in the early stage of conversion to glasses. *J Non-Cryst Solids.* 1990;126(1–2):68–78. [https://doi.org/10.1016/0022-3093\(90\)91024-L](https://doi.org/10.1016/0022-3093(90)91024-L).
36. Huang X, Brazel CS. On the importance and mechanisms of burst release in matrix-controlled drug delivery systems. *J Control Release.* 2001;73(2–3):121–36. [https://doi.org/10.1016/S0168-3659\(01\)00248-6](https://doi.org/10.1016/S0168-3659(01)00248-6).
37. Batycky RP, Hanes J, Langer R, Edwards DA. A theoretical model of erosion and macromolecular drug release from biodegrading microspheres. *J Pharm Sci.* 1997;86(12):1464–77. <https://doi.org/10.1021/js9604117>.
38. Brazel CS, Peppas NA. Recent studies and molecular analysis of drug release from swelling-controlled devices. *STP Pharm Sci.* 1999;9:473–85.
39. Brazel CS, Peppas NA. Mechanisms of solute and drug transport in relaxing, swellable, hydrophilic glassy polymers. *Polymer.* 1999;40(12):3383–98. [https://doi.org/10.1016/S0032-3861\(98\)00546-1](https://doi.org/10.1016/S0032-3861(98)00546-1).
40. Bataille B, Ligarski K, Jacob M, Thomas C, Duru C. Study of the influence of spheronisation and drying conditions on the physicochemical properties of neutral spheroids containing Avicel PH-101 and lactose. *Drug Dev Ind Pharm.* 1993;19(6):653–71. <https://doi.org/10.3109/03639049309062973>.
41. Cosijns A, Vervaeet C, Luyten J, Mullens S, Siepmann F, Van Hoorebeke L, et al. Porous hydroxyapatite tablets as carriers for low-dosed drugs. *Eur J Pharm Biopharm.* 2007;67(2):498–506. <https://doi.org/10.1016/j.ejpb.2007.02.018>.
42. Narasimhan B, Peppas NA. Molecular analysis of drug delivery systems controlled by dissolution of the polymer carrier. *J Pharm Sci.* 1997;86(3):297–304. <https://doi.org/10.1021/js960372z>.
43. Patil P, Paradkar A. Porous polystyrene beads as carriers for self-emulsifying system containing loratadine. *AAPS PharmSciTech.* 2006;7(1):E199–205. <https://doi.org/10.1208/pt070128>.
44. Sing KSW, Everett DH, Haul RAW, Moscou L, Pierotti RA, Rouquerol J, et al. Reporting physisorption data for gas solid systems with special reference to the determination of surface-area and porosity (recommendations 1984). *Pure Appl Chem.* 1985;57:603–19. <https://doi.org/10.1351/pac198254112201>.
45. Ma J, Chen CZ, Wang DG, Hu JH. Synthesis, Characterization and in vitro bioactivity of magnesium-doped sol-gel glass and glass-ceramics. *Ceram Int.* 2011;37(5):1637–44. <https://doi.org/10.1002/ceat.200900495>.
46. Bryan PD, Hawkins KR, Stewart JT, Capomacchia AC. Analysis of chlortetracycline by high-performance liquid-chromatography with postcolumn alkaline-induced fluorescence detection. *Biomed Chromatogr.* 1992;6(6):305–10. <https://doi.org/10.1002/bmc.1130060612>.
47. Naidong W, Roets E, Busson R, Hoogmartens J. Separation of keto—enol tautomers of chlortetracycline and 4-epichlortetracycline by liquid chromatography on poly(styrene—divinylbenzene)copolymer. *J Pharm Biomed Anal.* 1990;8(8–12):881–9. [https://doi.org/10.1016/0731-7085\(90\)80137-E](https://doi.org/10.1016/0731-7085(90)80137-E).
48. Mohammed-Ali MAJ. Stability study of tetracycline drug in acidic and alkaline solutions by colorimetric method. *J Chem Pharm Res.* 2012;4:1319–26.
49. Lindsey ME, Meyer M, Thurman EM. Analysis of trace levels of sulfonamide and tetracycline antimicrobials in groundwater and surface water using solid-phase extraction and liquid chromatography/mass spectrometry. *Anal Chem.* 2001;73(19):4640–6. <https://doi.org/10.1021/ac010514w>.
50. Weimann A, Bojesen G, Nielsen P. Analysis of tetracycline, oxytetracycline and chlortetracycline in plasma extracts by electrospray tandem mass-spectrometry and by liquid chromatography. *Anal Lett.* 1998;31(12):2053–66. <https://doi.org/10.1080/00032719808005284>.